Studying Crystal Properties using the Electron Microscope

Anonymous
Department of Physics, University of Toronto, Toronto M5S 1A7, Canada
(Dated: March 22, 2016)

This experiment studied the lattice properties of various specimens using a transmission electron microscope. The lattice structure and parameter of an unknown sample was found by looking at the diffraction patterns of elements with the same lattice structure (face-centered cubic– abbreviated FCC); the unknown sample was identified to be copper. The Curie temperature T_c of nickel was found by heating up the nickel sample slowly and observing the temperature at which the domain walls disappeared. The observed T_c was slightly outside the uncertainty for the known value for pure nickel. It was also concluded that nickel displayed paramagnetic behaviour for $T \geq T_c$.

I. INTRODUCTION

A transmission electron microscope, which will be referred to TEM henceforth, operates by transmitting an electron beam through a very thin specimen. The electron behaves as a wave with wavelength λ, and the atoms in the crystal sample act like scattering centres. This scattering produces waves– resulting in constructive and destructive interference. In the constructive interference, the electron wave's amplitude will be greater than its initial. In the destructive interference, the waves will cancel out. The result is a diffraction pattern.

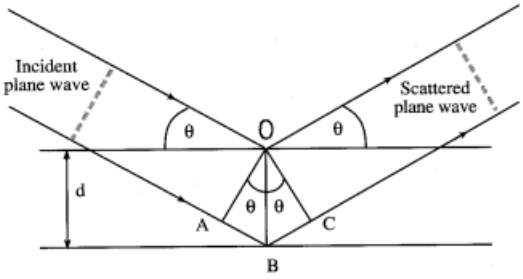

FIG. 1: Main components of a TEM compared to a light microscope [1].

From [Fig. 1], one can derive Bragg's law as shown in [Eq. 2]. Let θ be the angle of the incident electron beam relative to two parallel crystal planes with Miller indices (hkl).

d_{hkl} is the spacing between adjacent lattice planes with Miller indices (hkl) such that

$$d_{hkl} = \frac{a}{\sqrt{h^2 + k^2 + l^2}} \tag{1}$$

where a is the lattice parameter, and (hkl) are the Miller indices. The Miller indices represent which planes intersect the axes. For example, the (100) plane intersects only the $\vec{a}_1$ axis.

The constructive interference case results in a beam with higher intensity, while the destructive interference case results in a very small or even zero intensity beam. Constructive interference occurs when ABC is an integral multiple of the wavelength nλ. AB = BC = OBsin θ, 2OBsin θ = nλ and OB is just the distance between two parallel planes with Miller indices (hkl). Therefore, the condition for constructive interference in the scattering is given by

$$2d_{hkl} \sin\theta = n\lambda \tag{2}$$

The relation between the lattice plane spacing and the camera constant K for the diffraction pattern photographs is given by

$$d_{hkl} = n\left(\frac{K}{D}\right) \tag{3}$$

where n is a positive integer, D is the diameter of the ring, and d_{hkl} is the interplanar spacing. In [Eq. 2] and [Eq. 4], n represents the order of diffraction. However, in electron diffraction, it suffices to consider only the first order of diffraction (i.e. n = 1) because one can deal with higher order diffraction by using multiples of the Miller indices. For example, if one wants to study the second order diffraction from the (131) plane, one just needs to multiply by n = 2 to get the first order diffraction from the (262) plane. Therefore, the equation for the camera constant becomes

$$K = \frac{a \cdot D}{\sqrt{h^2 + k^2 + l^2}} \tag{4}$$

For ferromagnetic materials, the magnetic moments are aligned and parallel below T_c. Above T_c, the material undergoes a phase transition and the magnetic moments become disordered. For paramagnetic materials, the magnetic moments are aligned and parallel above T_c if there is a magnetic field present. Otherwise, the magnetic moments are disordered.

II. APPARATUS

The TEM used was the Hitachi EM III electron microscope. Unlike a light microscope, the illuminating source is an electron beam, instead of light. Instead of glass lenses, the TEM uses magnets to direct the electron beam. The accelerating voltage used to produce the electron beam was 75 kV. Throughout the experiment, the objective lens current remained constant at 101 mA while the projection lens remained at 71 mA. A firewire camera was used to record the diffraction patterns and domain images displayed on the plates. It was assumed to have an accuracy of 1 pixel. Each pixel represented 1/4.25 millimetres, resulting in an uncertainty of ±0.24mm.

All the samples in this experiment were metals with FCC structure: gold, aluminium, silver, and nickel. This allows us to look at the same set of (hkl) planes, which were (111), (200), (220), and (311) for elements with FCC structure. The diffraction pattern pictures were read using SciPy's ndimage module [2]. The intensity was then plotted against the x-axis

and the peak locations were found. Since the intensity plots are approximately symmetric, the distance between two peaks gives the diameter of a ring.

For observing nickel's domain structure, the TEM's field of view was changed. The nickel sample was heated slowly from 0.02 mV to 3 mV. The temperature was measured using a type R thermocouple with an uncertainty of $\pm 1.5\,^{\circ}\mathrm{C}$ or 0.25%. The relative uncertainty was used for the Curie temperature instead of the absolute.

Using a python program, the thermocouple voltages were converted into temperatures. Equivalently, the sample was heated from 276.89 K to 633.42 K. Pictures were taken around every 30 K. Pictures were also taken when the sample was cooling and while the domain walls reappeared as expected, the pictures did not provide any additional insight.

III. RESULTS

The intensity plots of the diffraction patterns for gold, aluminium, silver, and nickel are found in [Fig. 5] in the Appendix. THe intensity plot of the diffraction pattern for the unknown sample is shown below in [Fig. 2].

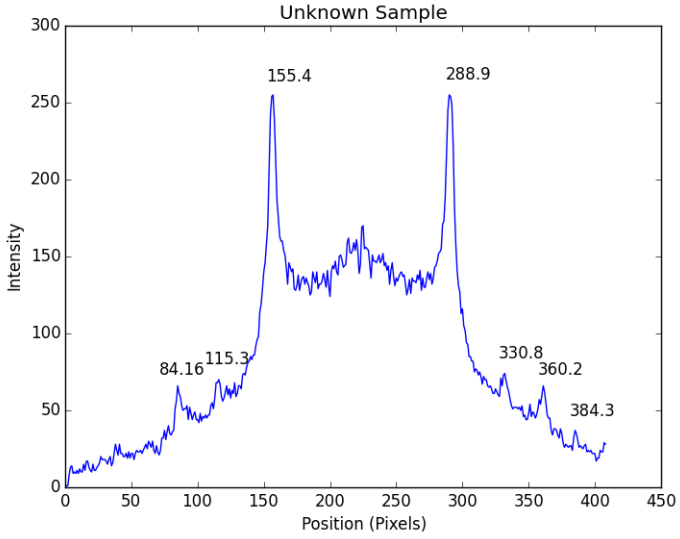

FIG. 2: Location of the intensity peaks in the unknown sample. Note that the peaks for the 4th ring are not well defined. This is because the 4th ring was very dim.

Naturally, in order to see the peaks in the 4th ring better, brighter pictures of the diffraction pattern were taken by increasing the current of the TEM. [Fig. 3] shows the locations of the intensity peaks of the 4th ring.

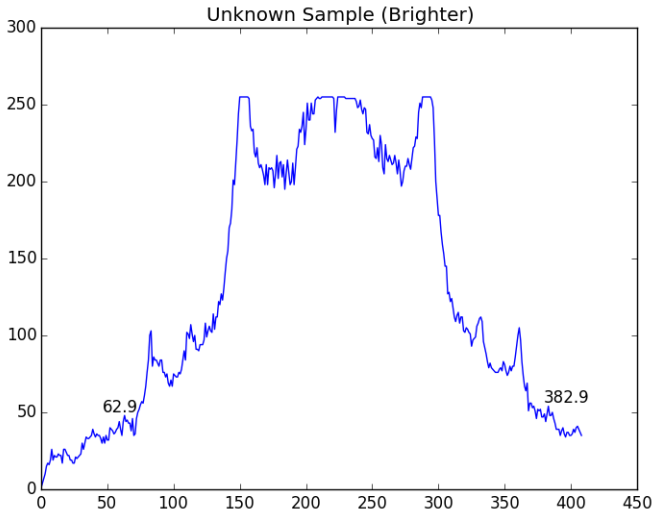

FIG. 3: A brighter diffraction pattern allows the intensity peaks in the 4th ring to appear.

The distance between the peak locations in the intensity plots above give the ring diameters. The diameters of the rings in the diffraction pattern corresponding to the (111), (200), (220), and (311) planes were found.

TABLE I: The diameter of the rings corresponding to the (111) plane.

Element	Diameter ($\pm$0.24mm)
Gold	27.47
Aluminum	28.18
Silver	25.55
Unknown	31.41

The diameters of the rings corresponding to the other planes are shown in [Table. II] in the Appendix.

Using the known lattice parameter of gold a = 0.4079 nm for calibration, and h = k = l = 1, the camera constant was found to be K = (1.617 $\pm$ 0.01) nm·mm using [Eq. 4]. The camera constant K was also calculated for the other rings as well but were not used; those results deviated slightly from the one obtained from the ring corresponding to the (111) plane. Since K is a known constant, one can rearrange [Eq. 4] for the lattice parameter a.

The lattice parameter of aluminium was found to be (0.3976 $\pm 3.5 \times 10^{-3}$) nm. The known value for aluminium is 0.4046 nm, which is within the uncertainty. Silver's lattice parameter was found to be (0.4386 $\pm 3.8 \times 10^{-3}$) nm. The known value for silver is 0.409 nm, which is outside the uncertainty. Since there is very small spread in the uncertainties for gold, aluminium, and silver, one can now calculate the lattice parameter of the unknown sample to determine what it is.

The unknown sample's lattice parameter was found to be a = (0.3567 $\pm 3.1 \times 10^{-3}$) nm. Copper has a lattice parameter of 0.3597 nm, so the unknown sample is identified as copper because it's within the uncertainty ($\pm 3.1 \times 10^{-3}$ nm).

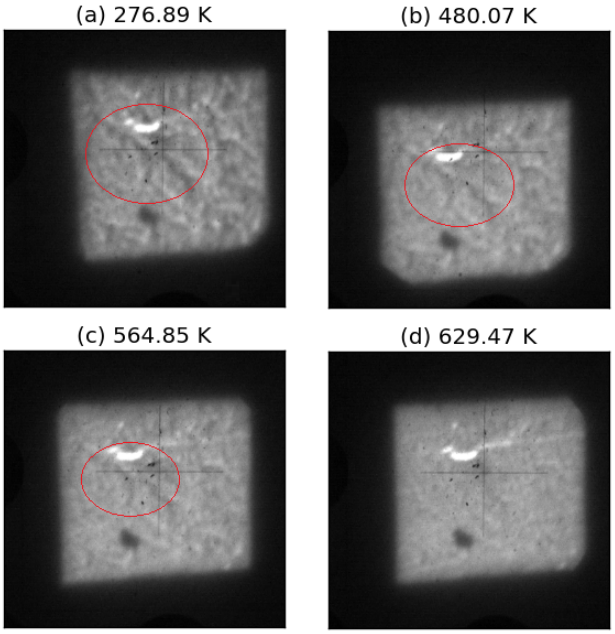

FIG. 4: The magnetic domain structures in nickel. The domain walls are not visible in (d) at the Curie temperature T_c = 629.47 K.

The domain walls that divide different orientations of the magnetic dipoles in nickel can be seen as the "bumps" in [Fig. 4]. The picture at 629.47 K is "smooth" when the domain walls disappear; all the magnetic dipoles have the same orientation as it increases beyond the Curie temperature, which is found to be $T_c = (629.47 \pm 1.6)$ K.

IV. DISCUSSION

In this experiment, the camera constant for any diffraction pattern photograph was calculated using a known value of gold's lattice parameter. Subsequently, this camera constant was used to find the lattice parameter and lattice structure of the unknown sample. However, it should be noted that one can only use the same set of Miller indices if the unknown sample also had a FCC structure. If the sample was, for example, body-centered cubic (BCC) instead, it would have planes with different Miller indices and one would not be able to use the same camera constant. One would need to recalibrate the camera constant using a known lattice parameter of another element with BCC structure, like chromium.

The Curie point of pure nickel is known to have an empirical value of $T_c = 627$ K. The value found in this experiment was $T_c = (629.47 \pm 1.6)$ K; which is slightly outside the uncertainty. Since Nickel is paramagnetic when $T \geq T_c$, the magnetic moments are ordered in the presence of an applied magnetic field produced by the TEM. This is consistent with what is seen in [Fig. 4]. The main sources of error in this part of the experiment were the infrequent pictures. The pictures were taken every 30 K; a third of this would be significantly better in determining T_c as the domain walls seemed to disappear before 629.47 K.

V. CONCLUSION

Using the transmission electron microscope to find the lattice parameter of the unknown sample a = $(0.3567 \pm 3.1 \times 10^{-3})$ nm, the unknown metal was identified to be copper which has lattice parameter a = 0.3597 nm.

After studying the domain structure of nickel, its Curie temperature was found to be $T_c = (629.47 \pm 1.6)$ K, which deviates slightly from the known Curie temperature of pure nickel T_c = 627 K.

[1] B. W. Statt, "Electron Microscope Lab Manual" (2015), 2-13
[2] Jones E, Oliphant E, Peterson P, et al. SciPy: Open Source Scientific Tools for Python, 2001-, http://www.scipy.org/[Online; accessed 2016-03-18].

VI. APPENDIX A

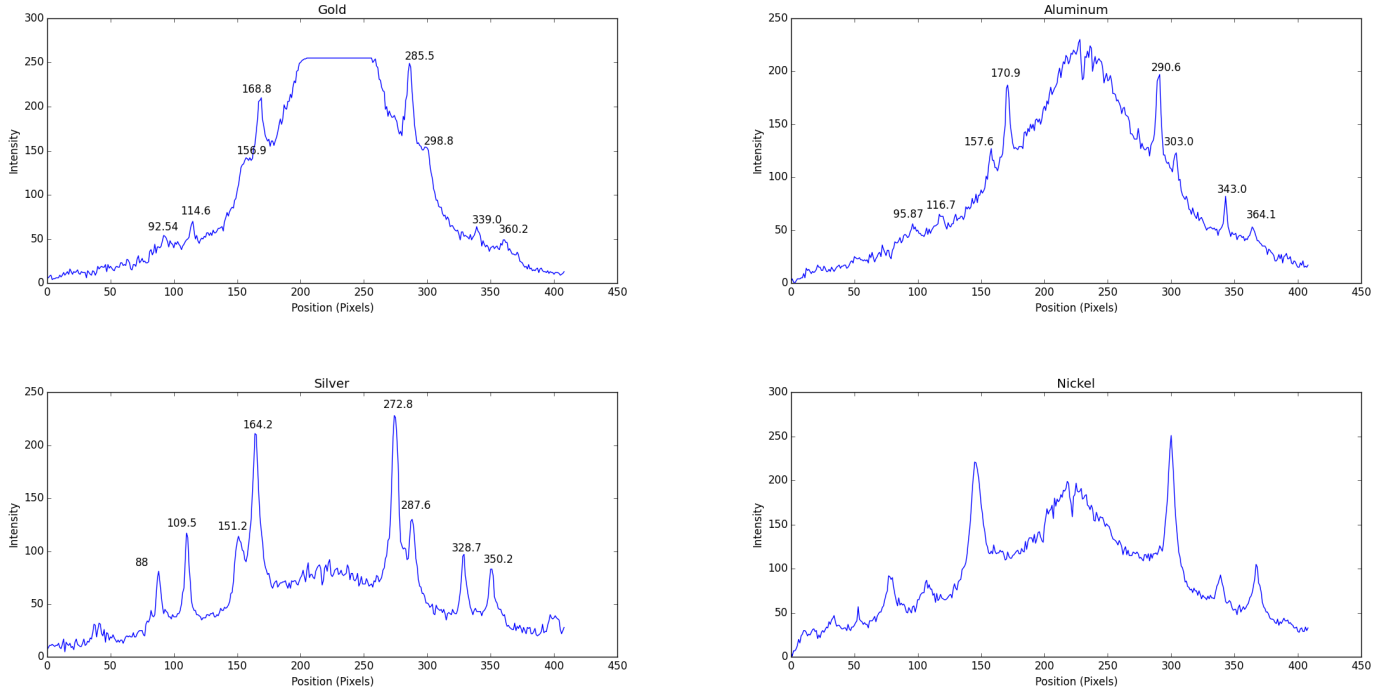

FIG. 5: Diffraction pattern intensity plots of gold, aluminium, silver, and pure nickel respectively. The peak locations are not labeled in the nickel intensity plot because it was not needed in the experiment.

TABLE II: The diameters of the rings corresponding to the (200), (220), and (311) planes.

Element	(200) (±0.24mm)	(220) (±0.24mm)	(311) (±0.24mm)
Gold	33.37	52.80	62.97
Aluminum	34.23	53.23	63.12
Silver	32.10	46.25	53.79
Unknown	50.71	64.95	75.29